Journal of Molecular Spectroscopy 263 (2010) 82–88

Contents lists available at ScienceDirect

Journal of Molecular Spectroscopy

journal homepage: www.elsevier.com/locate/jms

High resolution emission spectroscopy of the $A^2\Pi$–$X^2\Sigma^+$ (red) system of $^{12}C^{14}N$

R.S. Ram [a,*], L. Wallace [b], P.F. Bernath [a,c,d]

[a] Department of Chemistry, University of Arizona, Tucson, AZ 85721, USA
[b] Kitt Peak National Observatory, National Optical Astronomy Observatories, Tucson, AZ 85726, USA
[c] Department of Chemistry, University of Waterloo, Waterloo, Ont., Canada N2L 3G1
[d] Department of Chemistry, University of York, Heslington, York YO10 5DD, UK

ARTICLE INFO

Article history:
Received 24 May 2010
In revised form 11 July 2010
Available online 18 July 2010

Keywords:
Spectroscopy
Electronic spectra
Free radicals
Solar spectra
Carbon stars

ABSTRACT

The emission spectra of the $A^2\Pi$–$X^2\Sigma^+$ (red) system of $^{12}C^{14}N$ have been reinvestigated in the 3500–22 000 cm^{-1} region at high resolution using a Fourier transform spectrometer. In total, spectra of 63 bands involving vibrational levels up to $v' = 22$ of the $A^2\Pi$ state and $v'' = 12$ of the $X^2\Sigma^+$ ground state have been measured and rotationally analyzed providing an improved set of spectroscopic constants. The present measurements of the $\Delta v = -2$ sequence bands of $^{12}C^{14}N$ and those of $^{13}C^{14}N$ from Ram et al. (2010) [36] allow for a much improved identification of these two isotopologues in the near infrared spectra of carbon stars.

1. Introduction

CN is an important free radical. The spectrum of CN has been observed, for example, in solar and stellar atmospheres [1], circumstellar shells [2,3], the interstellar medium [4,5], in comets [6,7] and the integrated light of galaxies [8]. Recently CN lines were identified in the spectra of Red Rectangle nebula [HD 44179] along with CH and CH^+ [9]. The presence of CN in astronomical objects makes it a key probe of carbon and nitrogen abundance and isotopic ratios. Applications in astrophysics include the origin and abundances of the elements [10,11], the temperature of the microwave background radiation [12], the star formation process [8,13] and the origin of galaxies [14].

The characteristic red ($A^2\Pi$–$X^2\Sigma^+$) and violet ($B^2\Sigma^+$–$X^2\Sigma^+$) systems of CN are frequently observed in a wide variety of sources such as arcs, electrical discharges, flames and shock tubes with nitrogen, hydrogen and carbon containing species. CN was recently observed by graphite ablation using XeCl excimer laser radiation in a low-pressure nitrogen atmosphere [15]. The red and violet transitions extend from the near infrared to the ultraviolet, and CN is very persistent because of its strong bond. The electronic spectra were first observed about a century ago and many investigations have been carried out over the years using different experimental techniques. References to the previous electronic studies can be found in some recent papers on the red [16,17] and violet [17–19] systems.

CN was studied by the late S.P. Davis for several decades and a large number of measured line positions of the red system are tabulated in the Berkeley atlas [20]. In a previous high resolution study of the $A^2\Pi$–$X^2\Sigma^+$ transition Cerny et al. [21] recorded a high quality Fourier transform spectrum of the $\Delta v = -2$, $\Delta v = -1$, $\Delta v = 0$ and $\Delta v = 1$ sequences in the 4000–11 000 cm^{-1} region and provided a set of precise spectroscopic constants for the vibrational levels $v = 0$–4 of the ground ($X^2\Sigma^+$) and excited ($A^2\Pi$) states from the rotational analysis of 14 bands. Kotlar et al. [22] carried out a deperturbation analysis of the data in the Berkeley atlas and that of Cerny et al. [21] and gave a set of deperturbed spectroscopic constants for the $v = 0$–12 vibrational levels of the $A^2\Pi$ state and $v = 0$–8 vibrational levels of the $X^2\Sigma^+$ state. A study of the red system of CN was reported recently by Prasad and Bernath [16] using a jet-cooled corona-excited supersonic expansion source in which spectra in the 16 500–22 760 cm^{-1} range were recorded using a Fourier transform spectrometer. A total of 27 bands with $v' = 8$–21 of the $A^2\Pi$ state were measured. Although a large number of $A^2\Pi$ state vibrational levels were observed, the rotational structure consisted of only a few very low J lines belonging only to the lowest $A^2\Pi_{3/2}$–$X^2\Sigma^+$ sub-band because of the low rotational excitation temperature of the corona discharge source. Due to the lack of bands belonging to the $A^2\Pi_{1/2}$–$X^2\Sigma^+$ sub-band, a number of spectroscopic constants were fixed to estimated values. Several additional papers on the $A^2\Pi$–$X^2\Sigma^+$ transition have appeared recently which include the concentration modulation laser spectroscopy

* Corresponding author. Fax: +1 520 621 8407.
E-mail address: rram@u.arizona.edu (R.S. Ram).

0022-2852/$ - see front matter © 2010 Elsevier Inc. All rights reserved.
doi:10.1016/j.jms.2010.07.002

of the 2-0 band by Liu et al. [23], time-resolved Fourier transform spectroscopy of seven bands belonging to the $\Delta v = -3$ sequence by Civiš et al. [24] and the sub-Doppler Stark spectroscopy of the 1-0 band by Hause et al. [25].

Davis et al. [26] observed the vibration–rotation spectra in the $\Delta v = 1$ and $\Delta v = 2$ sequences of the ground state using a Fourier transform spectrometer. They measured the rotational lines in the 1-0, 2-1, 3-2, 4-3, 2-0, 3-1 and 4-2 bands and reported the equilibrium molecular parameters for the $X^2\Sigma^+$ ground state. In a more recent study, infrared laser spectroscopy was used to observe the fundamental 1-0 bands of $^{12}C^{14}N$ and $^{13}C^{14}N$ by Hempel et al. [27], and then Hübner et al. [28] reported the fundamental bands of the four isotopologues $^{12}C^{14}N$, $^{13}C^{14}N$, $^{12}C^{15}N$ and $^{13}C^{15}N$ using tunable diode laser absorption spectroscopy. Horká et al. [29] have observed the vibration–rotation spectra of the $\Delta v = 1$ bands from 1-0 to 9-8 using a Fourier transform spectrometer. The same spectra also contained the $\Delta v = -3$ sequence bands of the $A^2\Pi$–$X^2\Sigma^+$ transition reported by Civiš et al. [24]. In addition there are several microwave and millimeter wave studies of the $X^2\Sigma^+$ ground state [30–34] that provide measurements of the pure rotational transitions for the $v = 0$–10 vibrational levels.

Jørgensen and Larsson [35] have calculated the molecular opacities for the CN $A^2\Pi$–$X^2\Sigma^+$ transition. Rotational lines were calculated up to $J = 149.5$ for transitions between vibrational levels $0 \leqslant v' \leqslant 30$ and $0 \leqslant v'' \leqslant 30$ using available and extrapolated spectroscopic parameters for the $^{12}C^{14}N$, $^{13}C^{14}N$, $^{12}C^{15}N$, $^{13}C^{15}N$ isotopologues. The opacities were calculated for temperatures ranging from 1000 K to 6000 K.

In a recent publication we have reported on high resolution Fourier transform spectra of the $^{13}C^{14}N$ radical in the 4000–15 000 cm^{-1} region [36]. In total 22 bands of the $A^2\Pi$–$X^2\Sigma^+$ transition involving vibrational levels $v'' = 0$–5 and $v' = 0$–8 were measured and rotationally analyzed. An extensive set of spectroscopic constants and rotational line positions were provided for $^{13}C^{14}N$. Using these measurements many of the hither to unidentified lines in the near infrared spectra of carbon stars were identified as due to $^{13}C^{14}N$ [36].

In the present paper we report on the analysis of 63 vibrational bands involving vibrational levels $v'' = 0$–12 and $v' = 0$–22 of the ground and excited states of the red system of $^{12}C^{14}N$. The aim of the present study is to extend the measurements of bands in the $\Delta v = -2$ sequence to higher v and higher J values. These data are necessary for complete identification of the two isotopologues in the near infrared spectra of carbon stars which are rich in CN molecular lines. This study is also aimed at obtaining a more complete set of spectroscopic constants for the higher vibrational levels of the $A^2\Pi$ state. In our work the rotational lines were observed to higher J values than by Prasad and Bernath [16] in both sub-bands leading to improved spectroscopic constants. The previous microwave, infrared and near infrared measurements were added to the present data set and a more complete set of spectroscopic constants were determined for the $A^2\Pi$ state.

2. Experimental

The CN spectra used in the present analysis were recorded in several experiments from 1977 to 1992 using the Fourier transform spectrometer associated with the McMath–Pierce telescope of the National Solar Observatory located at Kitt Peak in Arizona. The sources used included a microwave discharge, active nitrogen afterglow, carbon arc, carbon tube furnace and an oxy-acetylene torch, and CN bands in the 1700 cm^{-1} to 30 000 cm^{-1} range were measured. Relative intensities of the bands vary by orders of magnitude from one source to another; therefore, the best bands from different sources were used in the analysis and all of the bands were brought to the same wavenumber scale using common rotational lines during the calibration of the spectra.

The carbon arc is a simple source in which carbon rods are used as electrodes. For the observation of CN bands the electrodes were enclosed in nitrogen gas at room temperature. In general arc sources are unstable and generate very noisy spectra but for a few short scans the arc was stable enough to record usable spectra. The excitation temperature of the arc source is of the order of 6000 °C resulting in lines with a large Doppler width. Spectra in the 8000–30 000 cm^{-1} range were recorded using several filter, beam splitter and detector combinations. The resolution in the arc experiments varied from 0.03 cm^{-1} to 0.05 cm^{-1}. The high temperature of the arc resulted in rotational lines excited up to very high J values. A few of these bands with very extensive rotational structure were used in the analysis.

CN bands were also recorded using a commercial carbon tube furnace (King furnace) which is operated at ~2500 °C. It was found that no additional carbon or nitrogen containing gas was required in the furnace to observe the spectra of CN. The furnace was operated at a pressure of about 75 Torr of helium gas in order to maintain a stable emission and avoid arcing. This source was used to record the spectrum in the 1700–11 400 cm^{-1} region at a resolution of 0.012 cm^{-1} by co-adding six scans. The furnace spectra always have a strong blackbody continuum that was subtracted before the line positions were measured.

A number of CN bands were measured from emission spectra recorded using a microwave electrodeless discharge lamp containing methane and nitrogen. The spectra in the 3500–20 000 cm^{-1} range were recorded in two parts. The 3500–12 000 cm^{-1} region was recorded using a visible beam splitter, InSb detectors and GaAs filters by co-adding eight scans at a resolution of 0.012 cm^{-1}. The 10 000–20 000 cm^{-1} region was recorded using the visible beam splitter, Si diode detectors and GG475 filters. The spectra observed in the microwave experiments were almost free from any contamination. The molecular lines observed from this source are sharper (line width of 0.045 cm^{-1} near 10 860 cm^{-1}) than the arc (line width of 0.13 cm^{-1}) and the carbon tube furnace (line width of 0.11 cm^{-1}). The spectra from this cooler source are suitable for analyzing the lines close to the band origins.

Several experiments were performed using a nitrogen afterglow (or active nitrogen) discharge source. This source was suitable for the observation of bands with high vibrational levels. The principal energy carriers in active nitrogen are the metastable triplet $A^3\Sigma_u^+$ and vibrationally excited ground state $X^1\Sigma_g^+$ of N_2. The N_2 $A^3\Sigma_u^+$ state is responsible for excitation of levels requiring more than ~4.5 eV energy while the vibrationally excited ground state participates in the excitation of lower energy levels. In these experiments CN was produced by the reaction of liquid-nitrogen-cooled active nitrogen and CH_4. Several experimental parameters such as the nitrogen pumping speed, gas pressure, gas temperature and particularly the liquid-nitrogen-cooling temperatures were adjusted in order to obtain a stable discharge with strong emission bands of CN. Although several experiments were carried out, the spectra recorded in two experiments which cover the 1700–11 200 cm^{-1} and 9000–29 600 cm^{-1} regions were selected for analysis. The 1700–11 200 cm^{-1} region was recorded using a CaF_2 beam splitter, InSb detectors and GaAs filters while the 9000–20 000 cm^{-1} region was recorded using a UV beam splitter, midrange Si diode detectors and no filters. The two experiments were performed by co-adding five and four scans, respectively, with the spectral resolution set at 0.01 cm^{-1} and 0.03 cm^{-1}. In these experiments the Doppler and pressure broadening are minimal (line width of 0.035 cm^{-1} near 10 860 cm^{-1}) and the spectra are free from any major contamination. These spectra have a low rotational temperature (~300 K) and much higher vibrational temperatures, and result in the observation of vibrational bands with

higher v's than the other sources. In fact we have been able to observe bands with vibrational levels up to $v' = 22$ of the $A^2\Pi$ and $v'' = 12$ of the $X^2\Sigma^+$ state from the afterglow spectra.

The line positions were extracted from the spectra using a data reduction program called PC-DECOMP developed by J. Brault. The peak positions were determined by fitting a Voigt line shape function to each spectral feature. The CN bands in the vicinity of 4000 cm^{-1} were calibrated using CO line measurements provided by Maki and Wells [37]. The spectra in the 5000–22 000 cm^{-1} region were calibrated using the Ar line measurements by Whaling et al. [38] as corrected by Sansonetti [39]. In the spectra where Ar lines are not present, the calibration was transferred from Ar lines to CN molecular lines. The spectra were brought to the same scale by transferring the calibration using common molecular lines. The precision of measurement is expected to be of the order of ±0.002 cm^{-1} or better for the stronger and unblended lines. The uncertainty in measurement of overlapped lines or weaker satellite branches is expected to be higher.

3. Observation

Our spectrum of $^{12}C^{14}N$ is full of molecular bands in the region of 3500–30 000 cm^{-1} that belong to the $A^2\Pi$–$X^2\Sigma^+$ (red) and $B^2\Sigma^+$–$X^2\Sigma^+$ (violet) electronic transitions. The analysis of the $B^2\Sigma^+$–$X^2\Sigma^+$ transition has been reported in a previous publication [19]. The $A^2\Pi$–$X^2\Sigma^+$ bands are located in the 3500–22 000 cm^{-1} region which appears complex because of overlapping of bands belonging to different sequences. Also, the intensity of different bands does not follow a regular trend making it difficult to make vibrational assignments without a proper rotational analysis. Therefore, most of the bands with sufficient intensity were measured and rotationally analyzed. In total sixty-three bands involving vibrational levels with $v'' = 0$–12 in the ground state and $v' = 0$–22 in the excited state were rotationally analyzed. These bands belong to vibrational sequences from $\Delta v = -2$ to $\Delta v = 11$. We have identified 12 branches in the strong bands including six satellite branches arising due to the spin-splitting in the ground state. However, in the high vibrational bands some of the branches (mainly satellite branches) could not be measured because of their weak intensity or relatively small splitting from the main lines.

3.1. The $\Delta v = -2, -1, 0, 1$ sequences

These bands are located in the 3500–11 000 cm^{-1} interval. The CN measurements in this region are particularly important for the solar spectrum and in the spectra of carbon stars. Some of the bands belonging to these sequences with vibrational levels up to $v = 4$ of the ground and excited states were rotationally analyzed by Cerny et al. [21]. We have extended their analysis to higher vibrational levels.

We have obtained the rotational analysis of 0-2, 1-3, 2-4, 3-5, 4-6, 5-7 and 6-8 bands of the $\Delta v = -2$ sequence of the $A^2\Pi$–$X^2\Sigma^+$ transition compared to the 0-2, 1-3 and 2-4 bands analyzed by Cerny et al. [21]. Additional higher vibrational bands fall below the filter cutoff in the experiment. The new 3-5, 4-6, 5-7 and 6-8 bands of the $\Delta v = -2$ sequence analyzed in the present work have R_2 heads near 4489, 4289, 4090 and 3892 cm^{-1}. We have obtained the rotational analysis of the 0-1, 1-2, 2-3, 3-4, 4-5, 6-7, 7-8 and 8-9 bands of the $\Delta v = -1$ sequence compared to the 0-1, 1-2, 2-3 and 3-4 bands analyzed by Cerny et al. [21]. In the $\Delta v = 0$ sequence we have obtained the rotational analysis of the 0-0, 1-1, 2-2, 3-3, 4-4, 5-5, 6-6 and 7-7 bands. Higher vibrational bands of this sequence fall under much stronger bands of the $\Delta v = -1$ sequence and were not analyzed. We have identified rotational lines with higher J values than those observed by Cerny et al. [21]. For example, we have identified rotational lines up to $J = 84.5$, 76.5 and 72.5 in the 0-2, 1-3 and 2-4 bands compared to lines with $J = 64.5$, 59.5 and 53.5, respectively, observed by Cerny et al. [21]. We have identified rotational lines up to $J = 97.5$ in the 0-1 band and up to $J = 104.5$ in the 0-0 band.

We have obtained the rotational analysis of the 1-0, 2-1 and 3-2 bands of the $\Delta v = 1$ sequence. These bands were also rotationally analyzed by Cerny et al. [21]. The location of the 4-3 band falls near 10 000 cm^{-1} where the detector response is low. We, therefore, did not attempt to analyze any higher vibrational bands in the $\Delta v = 1$ sequence.

3.2. The $\Delta v = 2, 3, 4, 5$ and 6 sequences

The $\Delta v = 2$ and $\Delta v = 3$ sequence bands are stronger in intensity than the $\Delta v = 1$ bands because of favorable Franck–Condon factors. We have obtained the rotational analysis of the 2-0, 3-1, 4-2, 5-3

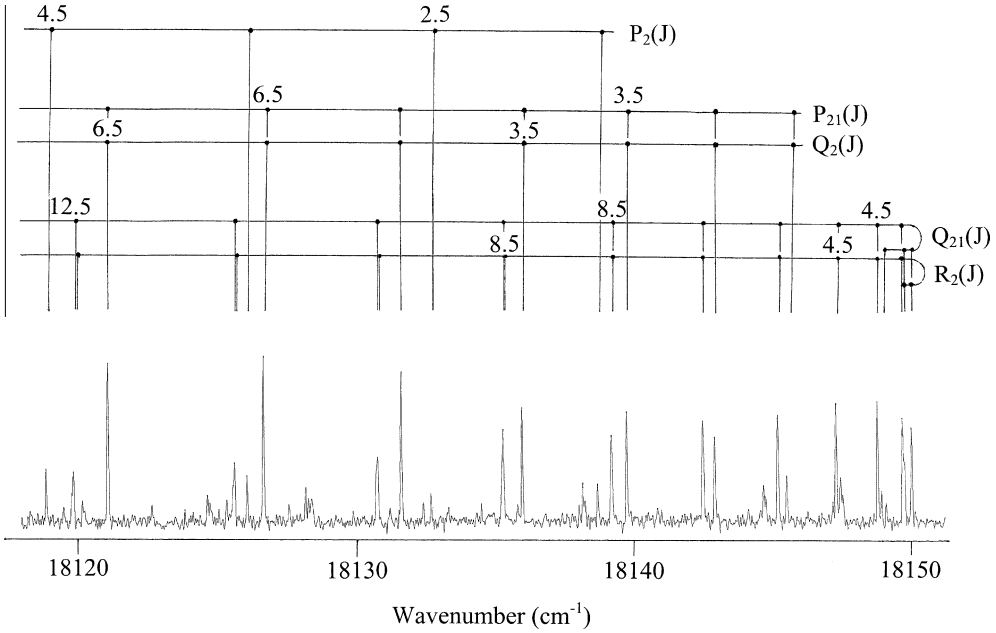

Fig. 1. A part of the spectrum of 18-10 band near the R_2 head of the $A^2\Pi$–$X^2\Sigma^+$ system of $^{12}C^{14}N$.

and 6-4 bands of the $\Delta v = 2$ sequence and 3-0, 4-1, 5-2 and 6-3 bands of the $\Delta v = 3$ sequence. We have also noticed that the intensity of higher vibrational bands of the higher Δv sequences increases with v, peaks and then slowly decreases. For example in the $\Delta v = 4$ sequence the intensity of bands varies as, 4-0 < 5-1 < 6-2 ≈ 7-3 > 8-4 > 9-5 band. This type of gradual intensity change is consistent with the Franck–Condon factors reported by Prasad and Bernath [16, see Table VIII].

We have obtained the rotational analysis of the 4-0, 5-1, 6-2 and 8-4 bands of the $\Delta v = 4$ sequence and the 8-3, 9-4, 10-5, 11-6 and 12-7 bands of the $\Delta v = 5$ sequence. Although we have observed the 7-1, 8-2, 9-3, 10-4, 11-5, 12-6, 13-7 and 14-8 bands of the $\Delta v = 6$ sequence in our spectra, we have measured and included the rotational lines only of the 13-7 band because the rotational lines of the lower vibrational bands can be calculated from the constants obtained from other bands.

3.3. The $\Delta v = 7$, 8, 9, 10 and 11 sequences

We have obtained the rotational analysis of the 14-7, 15-8 and 17-10 bands of the $\Delta v = 7$ sequence and 14-6, 15-7, 16-8 and 18-10 bands of the $\Delta v = 8$ sequence. A part of the 18-10 band showing some low J lines in the head-forming branches of the $A^2\Pi_{1/2}$–$X^2\Sigma^+$ sub-band has been provided in Fig. 1. As can be seen, the R_2 and Q_{21} branches which overlap at lower N values, gradually split for higher N values. We have also obtained the rotational analysis of the 16-7, 17-8, 18-9 and 19-10 bands of the $\Delta v = 9$ sequence, the 20-10, 21-11 and 22-12 bands of the $\Delta v = 10$ sequence and the 21-10 and 22-11 bands of the $\Delta v = 11$ sequence. Although the 22-11 band is much weaker in intensity than the other bands analyzed and only a few stronger branches (R_1, Q_1, Q_2) could be picked, the inclusion of this band is important for the determination of the term values for the $v' = 22$ vibrational level of the $A^2\Pi$ state. In the absence of this band the term value for the $v'' = 12$ of the ground state would need to be fixed to the value determined in our paper on the $B^2\Sigma^+$–$X^2\Sigma^+$ transition [19].

Rotational analysis of these bands indicates that the $v = 0$ vibrational level of the $A^2\Pi$ state is unaffected by perturbation over the observed range of J values up to $J = 104.5$. For $v = 1$ for which we have observed rotational line up to $J = 106.5$, local perturbations have been observed at $J = 91.5$ of $A^2\Pi_{3/2}$ (e) and $J = 77.5$ of $A^2\Pi_{3/2}$ (f) component. The energy levels of the $A^2\Pi_{1/2}$ component of this vibrational level are not perturbed. The $v = 2$ vibrational level of the $A^2\Pi$ state is not affected by perturbations over the observed

Table 1
Spectroscopic constants (in cm^{-1}) for the $A^2\Pi$ electronic state of $^{12}C^{14}N$.

Constants	$v = 0$	$v = 1$	$v = 2$	$v = 3$	$v = 4$	$v = 5$
T_v	9115.685528(63)	10903.41302(16)	12665.56754(17)	14402.13997(13)	16113.12051(13)	17798.49624(17)
A_v	−52.65441(13)	−52.58077(35)	−52.50525(35)	−52.43232(23)	−52.35628(18)	−52.28968(27)
$A_{Dv} \times 10^4$	−2.2011(23)	−2.1988(66)	−2.211(10)	−1.9609(63)	−1.8628(61)	−1.417(11)
$A_{Hv} \times 10^9$	5.005(32)	5.863(61)	7.96(17)	4.697(52)	4.342(59)	−5.86(20)
B_v	1.707138348(90)	1.68986159(25)	1.67254028(41)	1.65516958(24)	1.63775137(26)	1.62028779(46)
$D_v \times 10^6$	6.144621(90)	6.15564(11)	6.16896(24)	6.18163(11)	6.19826(13)	6.22232(22)
$H_v \times 10^{12}$	3.9082(94)	3.539(11)	3.393(31)	2.720(11)	2.410(12)	2.863(23)
$q_v \times 10^4$	−3.87333(56)	−3.9633(19)	−4.0548(36)	−4.1329(18)	−4.2559(29)	−4.3526(58)
$q_{Dv} \times 10^8$	0.96942(86)	1.0617(31)	1.1430(95)	1.1061(24)	1.2041(33)	1.087(12)
$p_v \times 10^3$	8.3761(46)	8.475(15)	8.363(21)	8.139(11)	8.067(12)	8.079(19)
$p_{Dv} \times 10^7$	−2.8351(88)	−3.485(31)	−3.430(76)	−2.555(28)	−2.110(34)	−5.63(12)
	$v = 6$	$v = 7$	$v = 8$	$v = 9$	$v = 10$	$v = 11$
T_v	19458.25781(20)	21092.46257(48)	22700.05189(42)	24283.17984(34)	25840.12176(38)	27371.20555(72)
A_v	−52.24815(36)	−52.34309(85)	−50.65974(77)	−51.45738(74)	−51.42868(84)	−51.3129(15)
$A_{Dv} \times 10^4$	−0.769(18)	−5.56(11)	1.412(94)	−3.724(40)	−3.514(51)	−2.55(26)
$A_{Hv} \times 10^7$	−0.0103(18)	4.70(11)	−9.92(11)	0.202(14)	0.351(24)	−1.43(41)
B_v	1.60279809(67)	1.5851661(51)	1.5676908(52)	1.5497800(14)	1.5319136(17)	1.513983(11)
$D_v \times 10^6$	6.25678(36)	5.629(12)	5.169(18)	6.3091(12)	6.3133(14)	6.207(34)
$H_v \times 10^9$	0.003547(44)	—	−1.219(18)	0.00363(22)	—	—
$q_v \times 10^4$	−4.629(12)	5.17(10)	6.954(84)	−5.052(15)	−5.067(10)	−5.421(79)
$q_{Dv} \times 10^6$	0.01702(19)	0.908(26)	−1.914(23)	0.02781(97)	—	—
$p_v \times 10^1$	0.08062(30)	0.0964(11)	1.3918(15)	0.20682(61)	0.15579(72)	0.1487(13)
$p_{Dv} \times 10^4$	0.000841(74)	−0.4120(47)	−2.8234(98)	−0.04372(60)	−0.01446(90)	—
$P_{Hv} \times 10^7$			2.241(16)			
	$v = 12$	$v = 13$	$v = 14$	$v = 15$	$v = 16$	$v = 17$
T_v	28876.36780(86)	30355.55269(82)	31808.62768(61)	33235.49713(49)	34636.00013(59)	36009.8738(24)
A_v	−51.1664(16)	−51.0043(14)	−50.8025(10)	−50.60738(84)	−50.38305(99)	−50.5253(39)
$A_{Dv} \times 10^3$	−0.390(16)	−0.2729(91)	−0.446(10)	−0.3250(59)	−0.2443(65)	−1.226(50)
B_v	1.496057(13)	1.477919(11)	1.459614(10)	1.4412984(64)	1.4229173(67)	1.404833(55)
$D_v \times 10^6$	6.371(38)	6.311(30)	6.328(32)	6.390(16)	6.556(16)	5.66(22)
$q_v \times 10^3$	−0.587(16)	−0.5079(87)	−0.6974(85)	−0.6738(61)	−0.5707(58)	−.2.91(26)
$p_v \times 10^2$	1.476(21)	1.321(14)	1.747(14)	1.4810(95)	1.236(10)	−1.83(10)
	$v = 18$	$v = 19$	$v = 20$	$v = 21$	$v = 22$	
T_v	37357.20745(66)	38677.42503(83)	39970.4620(11)	41235.86273(90)	42473.3644(15)	
A_v	−49.86343(92)	−49.49166(88)	−49.1746(20)	−48.7600(11)	−48.39846(86)	
$A_{Dv} \times 10^4$	−3.383(70)	−2.513((67)	−6.10(41)	−5.59(15)	—	
$A_{Hv} \times 10^6$	—	—	2.810(75)	—	—	
B_v	1.3853109(68)	1.3664052(86)	1.347266(18)	1.327212(12)	1.307826(25)	
$D_v \times 10^6$	6.553(18)	6.662(23)	4.825(62)	5.988(39)	7.102(65)	
$q_v \times 10^3$	−0.6779(82)	−0.5890(56)	0.127(14)	−1.153(12)	−0.6752(83)	
$p_v \times 10^2$	1.508(12)	1.6932(99)	0.362(30)	2.845(17)	1.537(15)	
$p_{Dv} \times 10^5$	—	—	−1.99(17)	—	—	

Note: Numbers quoted in parentheses are one standard deviation error in the last digits.

range of J values. Most of the higher vibrational levels are affected by local perturbations. The perturbations observed in the $v = 3, 4, 5, 6, 7, 8$ and 9 vibrational levels can be clearly seen in the observed–calculated differences corresponding to perturbed levels. For higher vibrational levels for which data were taken from the cooler spectra recorded using the active nitrogen source, the lines were observed only up to medium J values. For these levels no clear evidence of perturbations is observed from the fit, except for $v = 17$ and 18 vibrational levels of the $A^2\Pi$ state. For the $v = 17$ vibrational level lines with $J < 6.5$ of the $A^2\Pi_{3/2}$ (e) almost all the lines of the $A^2\Pi_{3/2}$ (f) and lines with $J > 7.5$ of the $A^2\Pi_{1/2}$ (f) spin component are affected by perturbations. For $v = 18$, $J > 14.5$ of $A^2\Pi_{3/2}$ (e) and $J = 8.5$ of $A^2\Pi_{3/2}$ (f) are affected by perturbations. The perturbation observed in the $v = 11$ vibrational level of the $X^2\Sigma^+$ state during the analysis of the $B^2\Sigma^+$–$X^2\Sigma^+$ transition [19] has been confirmed from the analysis of the 19-11 and 21-11 bands of the red system. The lines affected by perturbations were given lower weights or were deweighted in the final fit.

4. Analysis and discussion

The $A^2\Pi$ state of CN is inverted and an energy level diagram for the $A^2\Pi_i$–$X^2\Sigma^+$ electronic transition can be found in the paper by Cerny et al. [21]. Because of the large spin–orbit splitting in the $A^2\Pi_i$ state each band is split into two sub-bands $A^2\Pi_{3/2}$–$X^2\Sigma^+$ and $A^2\Pi_{1/2}$–$X^2\Sigma^+$ with the first sub-band being lower in wavenumber. These two sub-bands consist of R_1, P_1, Q_1 and R_2, P_2, Q_2 for the main branches. The presence of significant spin-splitting in the ground state results in the observation of additional R_{12}, P_{12}, Q_{12} and R_{21}, P_{21}, Q_{21} satellite branches. In the strong bands, all of the 12 branches have been measured and included in the analysis. In some weaker bands some of the satellite branches could not be identified because of their weaker intensity or overlapping from the main branches.

In order to determine rotational constants, the measured wavenumbers of the observed lines of different bands were fitted with the effective N^2 Hamiltonian of Brown et al. [40]. The matrix elements for the of this Hamiltonian for the $X^2\Sigma^+$ and $^2\Pi$ states are provided for example by Douay et al. [41] and Amiot et al. [42]. The lines in each of the vibrational bands were initially fitted separately using a non-linear least-squares procedure. In the final fit the measurements of all the bands were combined and fitted simultaneously. The vibration–rotation and pure rotational measurements of previous studies were also combined with our present measurements. In particular the measurements of the fundamental band measured by Hübner et al. [28] by diode laser spectroscopy and new infrared observations of the 1-0 to 9-8 vibration–rotation bands made by Horká et al. [29] were added. However, the infrared measurements do not resolve the spin-splitting. In the case of Hübner et al. [28] the lines were averaged for the few partly resolved cases. The infrared vibration–rotation lines from the Fourier transform and diode laser measurement were given estimated errors of 0.005 cm^{-1} in the final fit. The microwave measurements were given estimated errors ranging from 2×10^{-6} to 5×10^{-6} cm^{-1} as quoted in the papers [30–34], except for a few blended lines.

The weights for the weaker and blended lines of the red system were chosen according to the signal-to-noise ratio and extent of blending. The inclusion of the infrared measurements with the current measurements of the red system improves the molecular constants for the excited $A^2\Pi$ state. Also, our observation of satellite branches for high J values in the red system results in a direct determination of the spin-splitting constants γ_v in the ground state. The constants for the $A^2\Pi_i$ and $X^2\Sigma^+$ states of $^{12}C^{14}N$ obtained in this fit are provided in Tables 1 and 2, respectively. The spectroscopic parameters T_v (except $v = 0$), B_v, D_v, H_v, γ_v and γ_{Dv} were determined in the $X^2\Sigma^+$ ground state. The spectroscopic parameters T_v, A_v, A_{Dv}, A_{Hv} B_v, D_v, H_v, γ_v, γ_{Dv}, q_v, q_{Dv}, p_v and p_{Dv} were determined in the $A^2\Pi$ state.

A list of measurements used in the determination of the spectroscopic constants along with the observed–calculated residuals is available as Supplement 1 and as part of the Ohio State University Molecular Spectroscopy Archives (http://msa.lib.ohio-state.edu/jmsa_hp.htm). The term values for the observed vibrational levels of the $A^2\Pi$ and $X^2\Sigma^+$ states were calculated using the spectroscopic constants obtained in the final fit. A list of calculated term values is available as Supplement 2.

The spectroscopic constants of Tables 1 and 2 have been have been used to evaluate equilibrium constants for the $A^2\Pi$ and $X^2\Sigma^+$ states of $^{12}C^{14}N$ using the following expressions:

$$G(v) = \omega_e\left(v+\frac{1}{2}\right) - \omega_e x_e\left(v+\frac{1}{2}\right)^2 + \omega_e y_e\left(v+\frac{1}{2}\right)^3 + \omega_e z_e\left(v+\frac{1}{2}\right)^4 \quad (1)$$

$$A_v = A_e + \alpha_{A1}\left(v+\frac{1}{2}\right) + \alpha_{A2}\left(v+\frac{1}{2}\right)^2 + \alpha_{A3}\left(v+\frac{1}{2}\right)^3 \quad (2)$$

$$B_v = B_e + \alpha_1\left(v+\frac{1}{2}\right) + \alpha_2\left(v+\frac{1}{2}\right)^2 + \alpha_3\left(v+\frac{1}{2}\right)^3 \quad (3)$$

$$\gamma_v = \gamma_e + \gamma_1\left(v+\frac{1}{2}\right) + \gamma_2\left(v+\frac{1}{2}\right)^2 + \gamma_3\left(v+\frac{1}{2}\right)^3 \quad (4)$$

The effects of interactions are clearly visible in the excited state. For example, the spin–orbit interaction constants of the $v = 5, 6, 7, 8$ and 9 vibrational levels are −52.2897, −52.2482, −52.3431,

Table 2
Spectroscopic constants (in cm^{-1}) for the $X^2\Sigma^+$ ground state of $^{12}C^{14}N$.

v	T_v	B_v	$D_v \times 10^5$	H_v	γ_v	γ_{Dv}
0	0.0	1.891090286(53)	0.6407602(86)	$6.2642(92) \times 10^{-12}$	$7.25396(39) \times 10^{-3}$	$-7.79(77) \times 10^{-9}$
1	2042.421301(80)	1.873665818(44)	0.6416393(86)	$5.9734(92) \times 10^{-12}$	$7.17132(56) \times 10^{-3}$	$-1.009(81) \times 10^{-8}$
2	4058.549355(76)	1.856187445(54)	0.6426270(89)	$5.6639(97) \times 10^{-12}$	$7.07993(86) \times 10^{-3}$	$-1.66(11) \times 10^{-8}$
3	6048.34453(12)	1.838652872(91)	0.643790(13)	$5.478(19) \times 10^{-12}$	$6.9799(10) \times 10^{-3}$	$-2.42(25) \times 10^{-8}$
4	8011.76775(12)	1.82105955(16)	0.645038(18)	$5.183(35) \times 10^{-12}$	$6.8637(11) \times 10^{-3}$	$-3.65(37) \times 10^{-8}$
5	9948.77690(12)	1.80340419(16)	0.646412(24)	$4.967(61) \times 10^{-12}$	$6.7204(11) \times 10^{-3}$	$-6.11(53) \times 10^{-8}$
6	11859.32877(14)	1.78568493(16)	0.647499(35)	–	$6.5408(12) \times 10^{-3}$	–
7	13743.37602(16)	1.76789886(16)	0.649217(57)	–	$6.3134(11) \times 10^{-3}$	–
8	15600.87072((20)	1.75004063(22)	0.650945(91)	–	$6.0119(13) \times 10^{-3}$	–
9	17431.75553(40)	1.73210130(20)	0.65227(48)	–	$5.6133(18) \times 10^{-3}$	–
10	19235.95985(58)	1.71404927(23)	0.66034(71)	–	$5.2323(22) \times 10^{-3}$	–
11	21013.2912(10)	1.695253(23)	0.575(14)	$-4.40(26) \times 10^{-9}$	$1.090(13) \times 10^{-2}$	–
12	22765.7171(18)	1.677751(38)	1.262(22)	$1.234(39) \times 10^{-8}$	$1.3348(21) \times 10^{-1}$	$-2.325(14) \times 10^{-4}$

Note: Numbers quoted in parentheses are one standard deviation error in the last digits.

−50.6597 and −51.4574 cm^{-1}. A sudden drop in the value of A_8 indicates the presence of strong perturbation for the $v' = 8$ vibrational level. A similar strong interaction was noticed for the $v' = 17$ vibrational level of the excited state. Because of perturbations in the higher vibrational levels of the $A^2\Pi$ state, their values with $v' \geqslant 5$ were given much lower weights when fitting for the equilibrium vibrational constants in the $A^2\Pi$ state. Surprisingly, the rotational constants of the excited vibrational levels are less affected, although the rotational constants corresponding to the $v' = 8$ and $v' \geqslant 17$ were given reduced weights. Although the ground state vibrational levels are less affected by perturbations, a perturbation was clearly observed in the $v'' = 11$ vibrational level of the ground state. The $v'' = 12$ vibrational level of the ground state is also affected by interactions as can be seen from the abnormal values of the spectroscopic constants. For example, the distortion constants D_v and the spin-splitting constant γ_v have abnormal magnitudes compared to those for the lower vibrational levels. The values for the vibrational levels with $v'' \geqslant 10$ were given reduced weights in the determination of the equilibrium constants for the $X^2\Sigma^+$ state. The equilibrium constants for the two states are provided in Tables 3 and 4. The excited state equilibrium rotational constants obtained from this work are $B_e = 1.7157672(15)\ cm^{-1}$, $\alpha_e = 0.0172489(23)\ cm^{-1}$ for the $A^2\Pi$ state and $B_e = 1.89978432(81)\ cm^{-1}$, $\alpha_e = 0.01737523(86)\ cm^{-1}$ for the $X^2\Sigma^+$ state. The values reported in brackets are estimated one standard deviation uncertainties in the last digits. The present equilibrium constants agree well with the equilibrium constants reported by Cerny et al. [21]. The equilibrium bond lengths for the excited $A^2\Pi$ and ground $X^2\Sigma^+$ states obtained using the B_e values determined above are 1.23304557(54) Å and 1.17180 719(25) Å, respectively.

CN is an astrophysical molecule and has been observed in large abundance in carbon stars. The possibility of determining the $^{12}C/^{13}C$ ratio from the measurement of the $A^2\Pi$–$X^2\Sigma^+$ (red) system of CN has been suggested by Wyller [43] and Fay and Wyller [44]. The spectra of the cool carbon stars provide very rich CN spectra which provide a stringent test for any available CN line list. Lines in the 2.0–2.5 μm region were previously used by Lambert et al. [45] for $^{12}C/^{13}C$ abundance analysis. Cerny et al. [21] have measured the 0-2, 1-3 and 2-4 bands of the red system located in this region. In our work we have obtained measurements for the additional 3-5, 4-6, 5-7 and 6-8 bands of the $\Delta v = -2$ sequence of $^{12}C^{14}N$ located to lower wavenumbers. The previous laboratory measurements for $^{13}C^{14}N$ bands were available only for wavenumbers greater than 9000 cm^{-1}. In a recent paper [36] we have reported new measurements in the 4000–9000 cm^{-1} region of the red system of $^{13}C^{14}N$. The completeness and improved frequency precision of our new line lists for $^{12}C^{14}N$ and $^{13}C^{14}N$ will aid in identification of blended features used in abundance analysis, determination of isotopic ratios, and the identification of bands of less abundant molecules in this spectral region, especially in the complex spectra of carbon stars.

Using the line list for $^{12}C^{14}N$ provided here and the $^{13}C^{14}N$ line list from Ram et al. [36] we have identified a large number of CN lines in the 4000–5000 cm^{-1} region for some carbon stars. A section of two carbon star spectra studied by Lambert et al. [45] is shown in Fig. 2 of Ram et al. [36]. This figure clearly shows that our new line lists provide a more complete set of identifications for both $^{12}C^{14}N$ and $^{13}C^{14}N$. An excellent wavenumber agreement between the stellar line positions and our new line lists was found.

Table 3
Equilibrium constants for the $A^2\Pi$ electronic state of $^{12}C^{14}N$.

Constants	$A^2\Pi$
T_e	9243.29599(53)
ω_e	1813.28845(66)
$\omega_e x_e$	12.77789(24)
$\omega_e y_e$	−0.001775(24)
A_e	−52.6964(14)
$\alpha_{A1} \times 10^2$	8.50(17)
$\alpha_{A2} \times 10^3$	−4.00(38)
$\alpha_{A3} \times 10^4$	3.87(14)
B_e	1.7157672(15)
$\alpha_1 \times 10^2$	−1.72489(23)
$\alpha_2 \times 10^5$	−1.526(60)
$\alpha_3 \times 10^7$	−9.08(35)
r_e (Å)	1.23304557(54)

Note: Values in parentheses are one standard deviation uncertainties in the last digits.

Table 4
Equilibrium constants for the $X^2\Sigma^+$ electronic state of $^{12}C^{14}N$.

Constants	$X^2\Sigma^+$
T_e	0.0
ω_e	2068.68143(69)
$\omega_e x_e$	13.12050(34)
$\omega_e y_e$	−0.005637(61)
$\omega_e z_e$	−0.0000849(36)
B_e	1.89978432(81)
$\alpha_1 \times 10^2$	−1.737523(86)
$\alpha_2 \times 10^5$	−2.414(24)
$\alpha_3 \times 10^7$	−5.11(19)
$\gamma_e \times 10^3$	7.2977(14)
$\gamma_1 \times 10^5$	−8.87(21)
$\gamma_2 \times 10^6$	4.29(70)
$\gamma_3 \times 10^6$	−1.326(62)
r_e (Å)	1.17180719(25)

Note: Values in parentheses are one standard deviation uncertainties in the last digits.

5. Summary

The emission spectra of the $A^2\Pi$–$X^2\Sigma^+$ electronic transition of $^{12}C^{14}N$ have been measured at high resolution in the 3500–22 000 cm^{-1} region using a Fourier transform spectrometer. Some 63 vibrational bands have been rotationally analyzed and the measurements have been combined with the previous pure rotation and vibration–rotation measurements to extract improved spectroscopic constants for vibrational levels up to $v' = 22$ and $v'' = 12$ of the excited and ground electronic states. These measurements have been very useful in identifying CN lines in the 2.5 μm region of the spectra of carbon stars.

Acknowledgments

We thank J. Wagner, C. Plymate and G. Ladd of the National Solar Observatory for assistance in recording the spectra. The National Solar Observatory is operated by the Association for Research in Astronomy, Inc., under contract with the National Science Foundation. The research described here was partially supported by funds from the NASA laboratory astrophysics program. Some support was also provided by the UK Engineering and Physical Sciences Research Council (EPSRC).

Appendix A. Supplementary data

Supplementary data for this article are available on ScienceDirect (www.sciencedirect.com) and as part of the Ohio State University Molecular Spectroscopy Archives (http://library.osu.edu/sites/msa/jmsa_hp.htm). Supplementary data associated with this article can be found, in the online version, at doi:10.1016/j.jms.2010.07.002.

References

[1] D.L. Lambert, J.A. Brown, K.H. Hinkle, H.R. Johnson, Astrophys. J. 284 (1984) 223–237.
[2] A. Wootten, S.M. Lichten, R. Sahai, P.G. Wannier, Astrophys. J. 257 (1982) 151–160.
[3] G.R. Wiedemann, D. Deming, D.E. Jennings, K.H. Hinkle, J.J. Keady, Astrophys. J. 382 (1991) 321–326.
[4] B.E. Turner, R.H. Gammon, Astrophys. J. 198 (1975) 71–89.
[5] D.M. Meyer, M. Jura, Astrophys. J. 297 (1985) 119–132.
[6] J.R. Johnson, U. Fink, H.P. Larson, Astrophys. J. 270 (1983) 769–777.
[7] N. Fray, Y. Bénilan, H. Cottin, M.-C. Gazeau, J. Crovisier, Planet. Space Sci. 53 (2005) 1243–1262.
[8] R. Riffel, M.G. Pastoriza, Astrophys. J. 659 (2007) L103–L106.
[9] L.M. Hobbs, J.A. Thorburn, T. Oka, J. Barentine, T.P. Snow, D.G. York, Astrophys. J. 615 (2004) 947–957.
[10] D.L. Lambert, Mon. Not. R. Astron. Soc. 138 (1968) 143–179.
[11] V.V. Smith, K.H. Hinkle, K. Cunha, B. Plez, D.L. Lambert, C.A. Pilachowski, B. Barbuy, J. Melendez, S. Balachandran, M.S. Bessell, D.P. Geisler, J.E. Hesserm, C. Winge, Astrophys. J. 124 (2002) 3241–3254.
[12] K.C. Roth, D.M. Meyer, I. Hawkins, Astrophys. J. 413 (1993) L67–L71.
[13] M. Wang, C. Henkel, Y.-N. Chin, J.B. Whiteoak, M.H. Cunningham, R. Mauersberger, D. Muders, Astron. Astrophys. 422 (2004) 883–905.
[14] M. Banerji, S. Viti, D.A. Williams, Astrophys. J. 703 (2009) 2249–2258.
[15] S. Acquaviva, M.L. De Giorgi, J. Phys. B: At. Mol. Opt. Phys. 35 (2002) 795–806.
[16] C.V.V. Prasad, P.F. Bernath, J. Mol. Spectrosc. 151 (1992) 459–473.
[17] B.D. Rehfuss, M. Suh, T.A. Miller, V.E. Bondybey, J. Mol. Spectrosc. 151 (1992) 437–458.
[18] C.V.V. Prasad, P.F. Bernath, J. Mol. Spectrosc. 156 (1992) 327–340.
[19] R.S. Ram, S.P. Davis, L. Wallace, R. Engleman, D.R.T. Appadoo, P.F. Bernath, J. Mol. Spectrosc. 237 (2006) 225–231.
[20] S.P. Davis, J.G. Phillips, The Red System ($A^2\Pi$–$X^2\Sigma^+$) of the CN Molecule, University of California Press, Berkeley, 1963.
[21] D. Cerny, R. Bacis, G. Guelachvili, F. Roux, J. Mol. Spectrosc. 73 (1978) 154–167.
[22] A.J. Kotlar, R.W. Field, J.I. Steinfeld, J.A. Coxon, J. Mol. Spectrosc. 80 (1980) 86–108.
[23] Y. Liu, C. Duan, H. Liu, H. Gao, Y. Guo, X. Liu, J. Lin, J. Mol. Spectrosc. 205 (2001) 16–19.
[24] S. Civiš, T. Šedivcová-Uhlíková, P. Kubelík, K. Kawaguchi, J. Mol. Spectrosc. 250 (2008) 20–26.
[25] M.L. Hause, G.E. Hall, T.J. Sears, J. Phys. Chem. A 113 (2009) 13342–13346.
[26] S.P. Davis, M.C. Abrams, M.L.P. Rao, J.W. Brault, J. Opt. Soc. Am. B 8 (1991) 198–200.
[27] F. Hempel, J. Röpcke, A. Pipa, B.P. Davies, Mol. Phys. 101 (2003) 589–594.
[28] M. Hübner, M. Castillo, P.B. Davies, J. Röpcke, Spectrochim. Acta A61 (2005) 57–60.
[29] V. Horká, S. Civišs, V. Špirko, K. Kawaguchi, Collect. Czech. Chem. Commun. 69 (2004) 73–89.
[30] T.A. Dixon, R.C. Woods, J. Chem. Phys. 67 (1977) 3956–3964.
[31] D.D. Skatrud, F.C. DeLucia, G.A. Blake, K.V.L.N. Sastry, J. Mol. Spectrosc. 99 (1983) 35–46.
[32] M.A. Johnson, M.L. Alexander, I. Hertel, W.C. Lineberger, Chem. Phys. Lett. 105 (1984) 374–379.
[33] H. Ito, K. Kuchitsu, S. Yamamoto, S. Saito, Chem. Phys. Lett. 186 (1991) 539–546.
[34] E. Klisch, T. Klaus, S.P. Belov, G. Winnewisser, E. Herbst, Astron. Astrophys. 304 (1995) L5–L8. private communication for unpublished data in the Ph.D. thesis of E. Klisch.
[35] U.G. Jørgensen, M. Larsson, Astron. Astrophys. 238 (1990) 424–434.
[36] R.S. Ram, L. Wallace, K. Hinkle, P.F. Bernath, Astrophys. J. Suppl. Ser. 188 (2010) 500–505.
[37] A.G. Maki, J.S. Wells, Wavenumber Calibration Tables, NIST Database [NIST SP-118; US Government Printing Office, Washington, DC], 1995.
[38] W. Whaling, W.H.C. Anderson, M.T. Carle, J.W. Brault, H.A. Zarem, J. Res. Natl. Inst. Stand. Technol. 107 (2002) 149–169.
[39] C.J. Sansonetti, J. Res. Natl. Inst. Stand. Technol. 112 (2007) 297–302.
[40] J.M. Brown, E.A. Colbourn, J.K.G. Watson, F.D. Wayne, J. Mol. Spectrosc. 74 (1979) 294–318.
[41] M. Douay, S.A. Rogers, P.F. Bernath, Mol. Phys. 64 (1988) 425–436.
[42] C. Amiot, J.-P. Maillard, J. Chauville, J. Mol. Spectrosc. 87 (1981) 196–218.
[43] A.A. Wyller, Astrophys. J. 143 (1966) 828–850.
[44] T.D. Fay, A.A. Wyller, Sol. Phys. 11 (1970) 384–387.
[45] D.L. Lambert, J.A. Brown, K.H. Hinkle, H.R. Johnson, Astrophys. J. 284 (1884) 223–237.